

NTU

Lecture 11

Fall 2001

Chen

Transition Metals

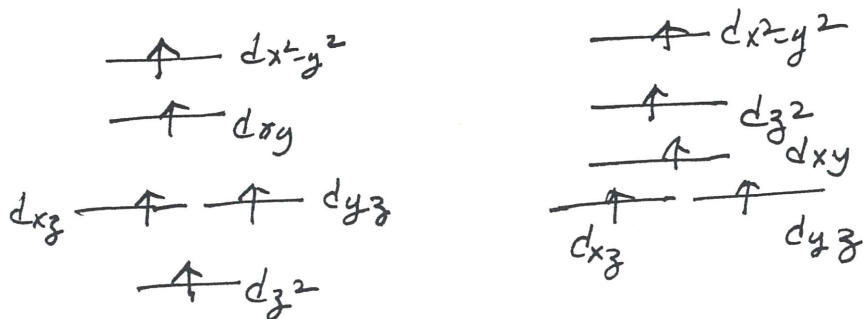
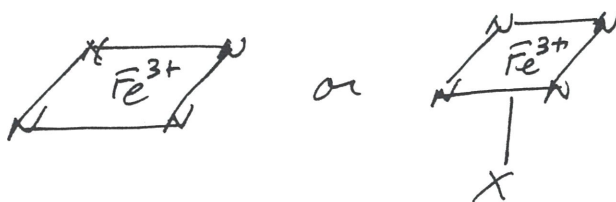
Free Ions of the Transition Metals

$3d^n$	Ti^{3+}	Spin Arrangement in Free Ion	Total Spin S
$3d^1$	Ti^{3+}	$\uparrow \text{--- ---}$	$\frac{1}{2}$
$3d^2$	V^{3+}	$\uparrow\uparrow \text{--- ---}$	1
$3d^3$	V^{2+} Cr^{3+}	$\uparrow\uparrow\uparrow \text{--- ---}$	$\frac{3}{2}$
$3d^4$	Cr^{2+} Mn^{3+}	$\uparrow\uparrow\uparrow\uparrow \text{---}$	2
$3d^5$	Mn^{2+} Fe^{3+}	$\uparrow\uparrow\uparrow\uparrow\uparrow$	$\frac{5}{2}$
$3d^6$	Fe^{2+} Co^{3+}	$\uparrow\downarrow \uparrow\uparrow\uparrow\uparrow$	2
$3d^7$	Co^{2+}	$\uparrow\downarrow \uparrow\downarrow \uparrow\uparrow\uparrow$	$\frac{3}{2}$
$3d^8$	Ni^{2+}	$\uparrow\downarrow \uparrow\downarrow \uparrow\downarrow \uparrow\uparrow$	1
$3d^9$	Cu^{2+}	$\uparrow\downarrow \uparrow\downarrow \uparrow\downarrow \uparrow\downarrow \uparrow$	$\frac{1}{2}$
$3d^{10}$	Zn^{2+} Cu^{1+}	$\uparrow\downarrow \uparrow\downarrow \uparrow\downarrow \uparrow\downarrow \uparrow\downarrow$	0

(2)

Ligand field or Crystal field will lift the degeneracy of d-orbitals, and affect the distribution of the spins among the d-orbitals
For example,

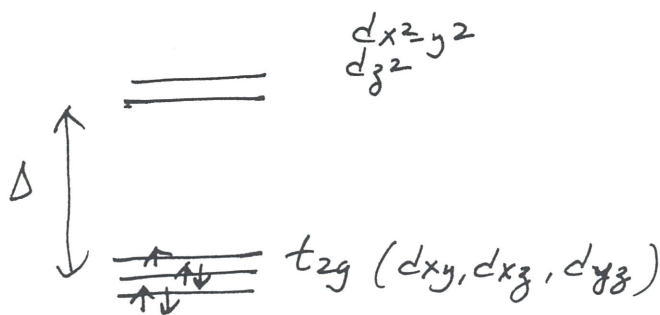
(1) for Fe^{3+} -porphyrin that is four-coordinate (uncapped) or five coordinate



High-spin
 $S = \frac{5}{2}$

High-spin
 $S = \frac{5}{2}$

(2) for Fe^{3+} -porphyrin that is six-coordinate



Strong crystal or ligand field

Δ large

Low-Spin $S = \frac{1}{2}$



Weak crystal field

Δ small compared with electron-electron repulsion

High-Spin $S = \frac{5}{2}$

Zero-field Splitting

If there is more than 1 unpaired electron spin, there will be magnetic interaction among the spins, and there will be a zero-field splitting.

The dipolar spin Hamiltonian takes the form

$$H_D = \vec{S} \cdot \tilde{D} \cdot \vec{S}$$

where \vec{S} is the total spin operator for the unpaired e's and \tilde{D} is the zero-field splitting tensor!

For 2 unpaired electron spins,

$$D_{xx} = \pm g^2 \beta^2 \left\langle \frac{r_{12}^2 - 3x_{12}^2}{r_{12}^5} \right\rangle$$

$$D_{xy} = \pm g^2 \beta^2 \left\langle \frac{-3x_{12}y_{12}}{r_{12}^5} \right\rangle$$

In the principal axes system of \tilde{D} ,

$$\begin{pmatrix} D_{xx} & D_{xy} & D_{xz} \\ D_{yx} & D_{yy} & D_{yz} \\ D_{zx} & D_{zy} & D_{zz} \end{pmatrix} \longrightarrow \begin{pmatrix} -X & 0 & 0 \\ 0 & -Y & 0 \\ 0 & 0 & -Z \end{pmatrix}$$

so that

$$H_D = -X S_x'^2 - Y S_y'^2 - Z S_z'^2$$

Now $X + Y + Z = 0$, so that only 2 of these quantities are independent!

Customary to define

$$D = \frac{1}{2}(X+Y)-Z$$

$$E = -\frac{1}{2}(X-Y)$$

Then

$$\begin{aligned} K_D &= -XS_{xx}^2 - YS_{yy}^2 - ZS_{zz}^2 \\ &= D(S_z^2 - \frac{1}{3}S^2) + E(S_x^2 - S_y^2) \end{aligned}$$

Will drop "prime" henceforth, remembering that D and E are always referred to principal axes of the zero-field splitting tensor (X, Y, Z)

Second-order Spin-orbit Energy

Aside from magnetic interactions among unpaired spins, spin-orbit coupling can lead to an indirect electron spin-spin coupling.

Spin-orbit energy to second order

$$= -\lambda^2 \sum_n \frac{\langle 0 | \vec{L} \cdot \vec{S} | n \rangle \langle n | \vec{L} \cdot \vec{S} | 0 \rangle}{E_n - E_0}$$

which could be rewritten as

$$H_{SO} = \hat{S} \cdot \underline{D} \cdot \hat{S}$$

(5)

$$\text{with } D_{ik} = -\lambda^2 \sum_n \frac{\langle \psi_0 | L_i | \psi_n \rangle \langle \psi_n | L_k | i \rangle}{E_n - E_0}$$

where $i, k = x, y, z$

For transition metals, spin-orbit contribution to D usually dominates!

Nevertheless, still the same spin Hamiltonian

$$H_{ZS} = D(S_z^2 - \frac{1}{3}S^2) + E(S_x^2 - S_y^2)$$

where we lump $H_D + H_{SO}$ together, so that D and E now include contributions from magnetic dipolar and spin-orbit interactions.

Some concrete examples

(i) $S = \frac{1}{2}$ $S_z = \pm \frac{1}{2}$ so that $\langle S_z^2 - \frac{1}{3}S^2 \rangle$

$$= \left\langle \frac{1}{4} - \frac{1}{3}S(S+1) \right\rangle$$

$$= \frac{1}{4} - \left[\frac{1}{3} \cdot \frac{1}{2} \left(\frac{3}{2} \right) \right] = 0$$

also $\langle S_x^2 \rangle = \langle S_y^2 \rangle = \frac{1}{4}$

So $H_{ZS} = 0$

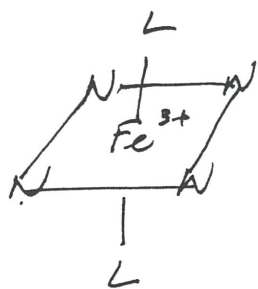
No ZS splitting for $S = \frac{1}{2}$

(6)

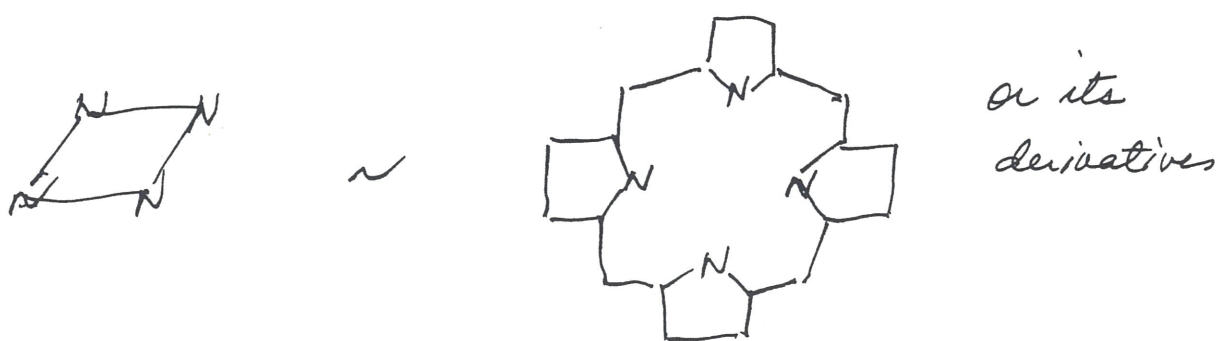
$$\text{and } H_S = H_T = \beta \vec{S} \cdot \vec{g} \cdot \vec{H}$$

g -tensor anisotropy due to spin-orbit coupling.

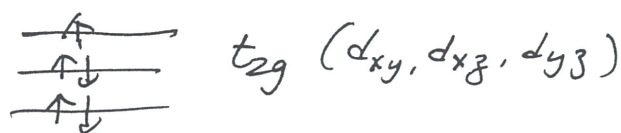
A good example would be low-spin d^5 , as for a six-coordinate Fe(III) porphyrin with strong-field axial ligands, schemically shown as



where



$$= \begin{array}{c} d_{x^2-y^2} \\ d_{z^2} \end{array} \quad (\text{eg})$$



or 1 unpaired electron in t_{2g} orbitals (O_h) octahedral
or 1 unpaired electron in d_{x^2}, d_{y^2} (degenerate) for square bipyramidal
Effective g -values : 3, 2, 1.5

(7)

(b) In contrast $S = \frac{5}{2}$

e.g. high spin Fe^{3+} -porphyrin

5 unpaired electrons: $(d_{xy}^1 d_{xz}^1 d_{yz}^1 d_{z^2}^1 d_{x^2-y^2}^1)$

- Exchange interaction among five unpaired spins
 $\Rightarrow S = \frac{5}{2}$ ground state

- But the unpaired electrons also interact magnetically via magnetic dipole-dipole interaction and via second-order spin-orbit coupling

Therefore $H_S = H_{ZS} + H_Z$

$$= D(S_z^2 - \frac{1}{3}S(S+1)) + E(S_x^2 - S_y^2)$$

$$+ \beta \vec{H} \cdot \vec{g} \cdot \vec{S}$$

For Fe-porphyrin

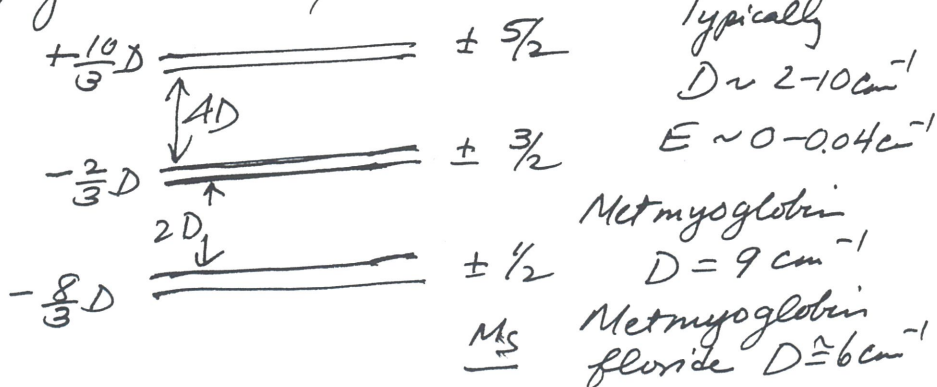
z + porphyrin plane; x, y in porphyrin plane.

For D_{4h} porphyrin, $E=0$, so $H_{ZS} = D(S_z^2 - \frac{1}{3}S(S+1))$

Since $\langle S_z^2 \rangle = M_S^2$ where $M_S = \pm \frac{5}{2}, \pm \frac{3}{2}, \pm \frac{1}{2}$

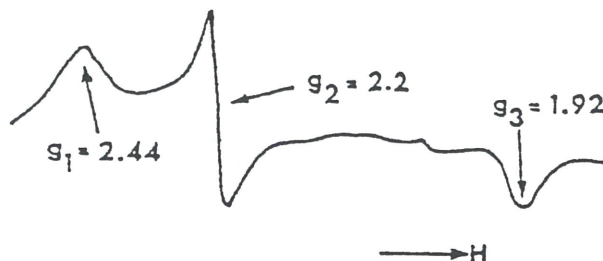
(projection of spin along porphyrin normal)

Energy levels
quadrupole splitting
for $E \approx 0$



(8)

- Low Temperature (4.2 K) EPR is the easiest and the most unequivalent way to determine the spin state of an iron heme in the ferric state.
-
- (1) Low-spin d⁵

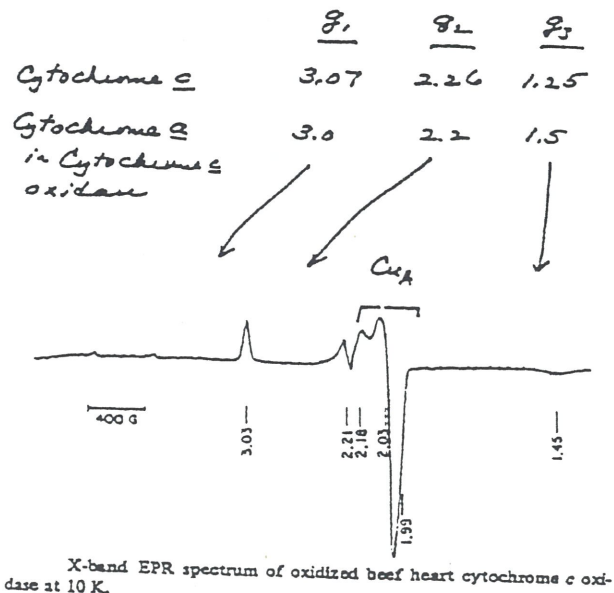


EPR of resting (oxidized) cytochrome P-450 before substrate is bound.

(2) Other low-spin hemes in hemoproteins

<i>g</i> -values of low-spin hemoproteins			
	g_1	g_2	g_3
Mb.OH	2.61	2.19	1.82
Mb.N ₃	2.8	2.25	1.75
Hb.OH	2.6	2.3	1.7
Hb.N ₃	2.82	2.2	1.70
Peroxidase.OH	2.36	2.12	1.67
Cytochrome c peroxidase	2.7	2.2	1.83
Cytochrome b ₅	3.03	2.23	1.93
Catalase.N ₃	2.80	2.18	1.74
	(2.53)	2.2	1.85
Catalase.CN	2.84	2.25	1.66
	2.56	2.31	1.81
	(2.43)	2.17	1.895

Mb is myoglobin and Hb is hemoglobin.

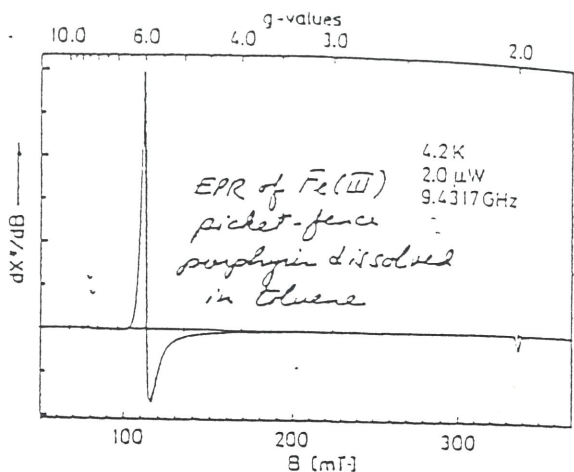
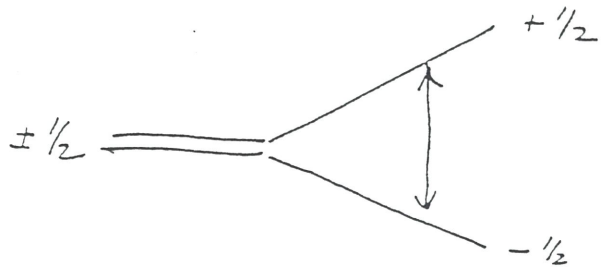


X-band EPR spectrum of oxidized beef heart cytochrome c oxidase at 10 K.

(3) High-spin heme centers

Hemoprotein	$\underline{g_1}$	$\underline{g_2}$	$\underline{g_3}$
Met Mb	5.9		2.0
Catalase	6.6	5.4	2.0
+F ⁻	6.5	5.5	2.0
+N ₃ ⁻	6.1	5.2	2.0
P-450	6.6	5.3	2.0

Conventional EPR only observed for $\pm \frac{1}{2}$ level, the so-called
Kramer doublet



$g_{eff} \approx 2$ when $\vec{H} \parallel z$ (along porphyrin normal)

6 when $\vec{H} \perp z$ (in porphyrin plane)

$$g_{xy}^{eff} = 6 \pm 24 \left(\frac{E}{D} \right) \text{ for deviation from axial symmetry}$$

Note that Fe^{3+} -porphyrins are usually observed near liquid helium temperatures, where essentially the lowest level is populated ($S_z = \pm \frac{1}{2}$ Kramer doublet if $D > 0$)

of course, for $D < 0$, $S_z = \pm \frac{5}{2}$ lowest occupied and no EPR is expected (!) at low temperatures.

Cytochrome α_3 6.0 2.0
in Cytochrome c oxidase

- (4) Recall for high-spin heme, conventional EPR arise from $m_s = \pm 1/2$ Kramer doublet:

$$\begin{cases} g \sim 6 \text{ when } \vec{H} \text{ is in porphyrin plane} \\ g \sim 2 \text{ when } \vec{H} \text{ is } \perp \text{ porphyrin plane} \end{cases}$$

When porphyrin has D_{4h} symmetry (axial), $E=0$ and $g=6.0$. When zero-field interaction has a rhombic component, i.e., $E \neq 0$, then

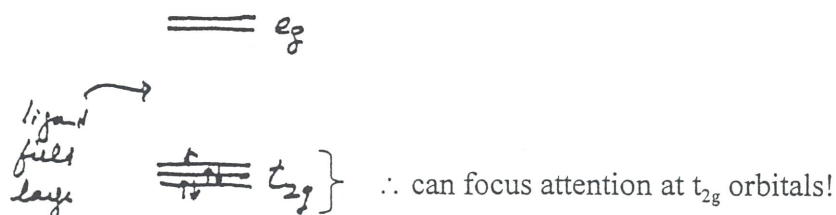
$$g_{\perp} = 6.0 \pm 24(E/D)$$

e.g. for $E \sim 0.04 \text{ cm}^{-1}$ $D \sim 10 \text{ cm}^{-1}$ (Cytochrome α_3 in cytochrome c oxidase)



$E \sim 0.04 \text{ cm}^{-1}$ is a relatively small rhombic distortion.

- (5) For low spin heme, deviation of g -values from 2.0023 arises from spin-orbital interaction.



At this level of approximation, problem is orbitally degenerate \Rightarrow John-Teller distortion to D_{2h} symmetry, which lifts degeneracy of 3 t_{2g} orbitals.

//

yz	$\frac{\uparrow}{\underline{\hspace{1cm}}}$	yz	$\frac{\uparrow\downarrow}{\underline{\hspace{1cm}}}$	yz	$\frac{\uparrow\downarrow}{\underline{\hspace{1cm}}}$
xz	$\frac{\uparrow\downarrow}{\underline{\hspace{1cm}}}$	xz	$\frac{\uparrow}{\underline{\hspace{1cm}}}$	xy	$\frac{\uparrow\downarrow}{\underline{\hspace{1cm}}}$
xy	$\frac{\uparrow\downarrow}{\underline{\hspace{1cm}}}$	xy	$\frac{\uparrow\downarrow}{\underline{\hspace{1cm}}}$	xy	$\frac{\uparrow}{\underline{\hspace{1cm}}}$

ground state

1st excited state

2nd excited state

$(d_{yz})^+$

$(d_{xz})^+$

$(d_{xy})^+$

← spin "up"

Spin-orbit interaction mixes these states

For example,

$$\Psi_1^+ = A_1(d_{yz})^+ + B_1(i)(d_{xz})^+ + C_1(d_{xy})^-$$

and $\Psi_1^- = -A_1(d_{yz})^- + B_1(i)(d_{xz})^- + C_1(d_{xy})^+$

More explicitly

$$\begin{aligned} \Psi_1^+ &= A_1(d_{yz})^+ + \frac{\langle d_{xz}^+ | -\lambda \vec{L} \cdot \vec{S} | d_{yz}^+ \rangle}{\varepsilon_{yz} - \varepsilon_{xz}} (d_{xz})^+ + \frac{\langle d_{xy}^- | -\lambda \vec{L} \cdot \vec{S} | d_{yz}^+ \rangle}{\varepsilon_{yz} - \varepsilon_{xy}} (d_{xy})^- \\ &= A_1(d_{yz})^+ + \frac{i\lambda}{2(\varepsilon_{yz} - \varepsilon_{xz})} (d_{xz})^+ + \frac{\lambda}{2(\varepsilon_{yz} - \varepsilon_{xy})} (d_{xy})^- \end{aligned}$$

where ε_{yz} , ε_{xz} , ε_{xy} are the energies of $(d_{yz})^\pm$, $(d_{xz})^\pm$, $(d_{xy})^\pm$ the so called "hole" states.

ε_{xy}	_____	$(d_{xy})^\pm$	spin-orbit interaction
ε_{xz}	_____	$(d_{xz})^\pm$	mixes these "hole" states
ε_{yz}	_____	$(d_{yz})^\pm$	

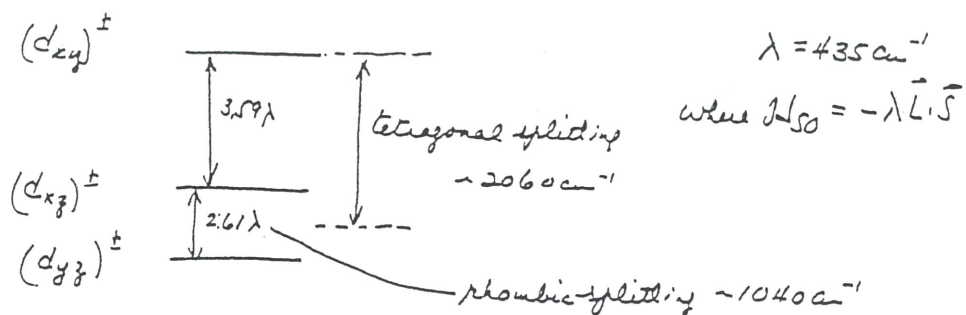
Similar final wavefunctions can be written for remaining two Kramer doublets.

For azidoferrithemoglobin (Hb, N₃), where $g_1 = 2.80$, $g_2 = 2.22$ and $g_3 = 1.72$

	i	Ai	Bi	Ci	
Kramer	1	0.973	-0.207	-0.097	$\sim(d_{yz})^\pm$
doublet	2	0.219	0.970	0.108	$\sim(d_{xz})^\pm$
	3	0.017	-0.126	0.990	$\sim(d_{xy})^\pm$

(13)

To fit g-values for azidoferrihemoglobin, requires



at 4.2 - 20 K, only $(d_{yz})^{\pm}$ Kramer doublet is populated!

Ref. F.S.Griffith, "Theory of Transition -Metal Ions" Cambridge University Press.
M. Kotani, Advances in Chem. Physics 7, 159 (1964)

(6) Since different axial ligands affect the tetragonal and rhombic splittings differently, the g-values for a low-spin heme can be used to infer the axial ligands.

The relation between EPR parameters and structure of low spin ferric heme compounds (taken from [1])

Compound	Axial ligands	g values		
Glycera Hb MeNH ₂	imid	RNH ₂	3.30	1.98
Leg Hb pyridine	imid	pyr	3.26	2.10
Cytochrome c	imid*	met	3.07	2.26
Bis imid heme	imid*	imid*	3.02	2.24
Bis imid* heme	imid*	imid*	2.80	2.26
MbOH	imid	OH ⁻	2.55	2.17
Cyt. P-450 _{cam}	imid*	RS ⁻	2.45	2.26
Cyt. c oxidase	imid*	imid*	3.0	2.2
				1.5

this approach was used to argue that cytochrome a in cytochrome c oxidase is six-coordinate with N from neutral imidazoles as axial ligands

A better approach to infer the axial ligands of hemes in hemoproteins is EXAFS.

EXAFS spectroscopy has provided the first direct, compelling evidence demonstrating that the proximal ligand to the heme in P-450 (in states 1-5) and chloroperoxidase (state 2 and 4) is a thiolate sulfur.

Ref. S.P. Cramer, J. H. Dawson, K.O. Hodgson and L. P. Hager, *J. Am. Chem. Soc.* 100, 7282 (1978).

Other spin systems

(c) High-spin d^6 and high-spin d^4
 e.g. high-spin Fe^{2+} e.g. Mn^{3+}

$$\boxed{\pm 2} \quad (4 \text{ unpaired electrons})$$

$$\pm 2 =$$

zero-field
splitting
for $D > 0$

$$\pm 1 =$$

$$0 =$$

No Kramer doublet

→ no conventional EPR!

(d) Low-spin d^6

e.g. Fe^{2+} -porphyrin in oxy Mb or reduced cytochrome a
 in Cytochrome c
 oxidase

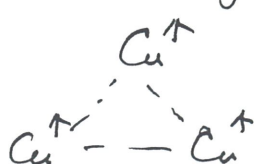
$$\boxed{\pm 0}$$

no EPR !

(e) $S = 3/2$, e.g. Co^{2+} (d^7);

Mo^{3+} in MoFe_3S_3 cluster
 $(4d^3)$

or ground state of ferromagnetically
coupled oxidized trinuclear Cu^{2+} cluster

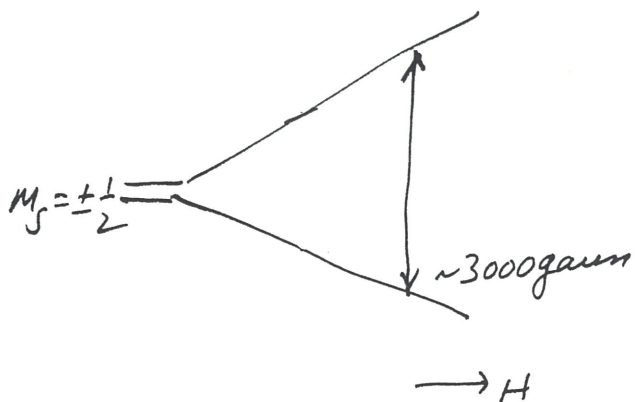


(in C-cluster of)
 PMMO

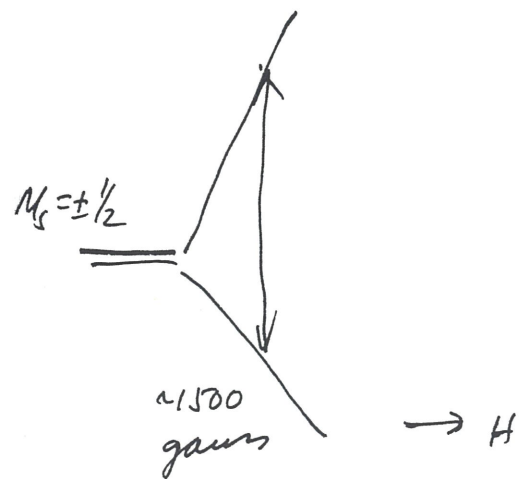
$\equiv \pm \frac{3}{2}$

zero-field splitting \rightarrow

$\equiv \pm \frac{1}{2}$ Kramer Doublet

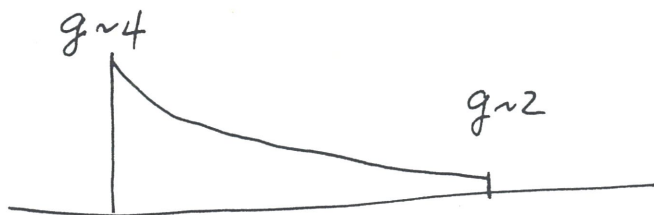


$g \approx 2$ when \vec{H} along z -axis
or \perp triangular plane
of trinuclear cluster



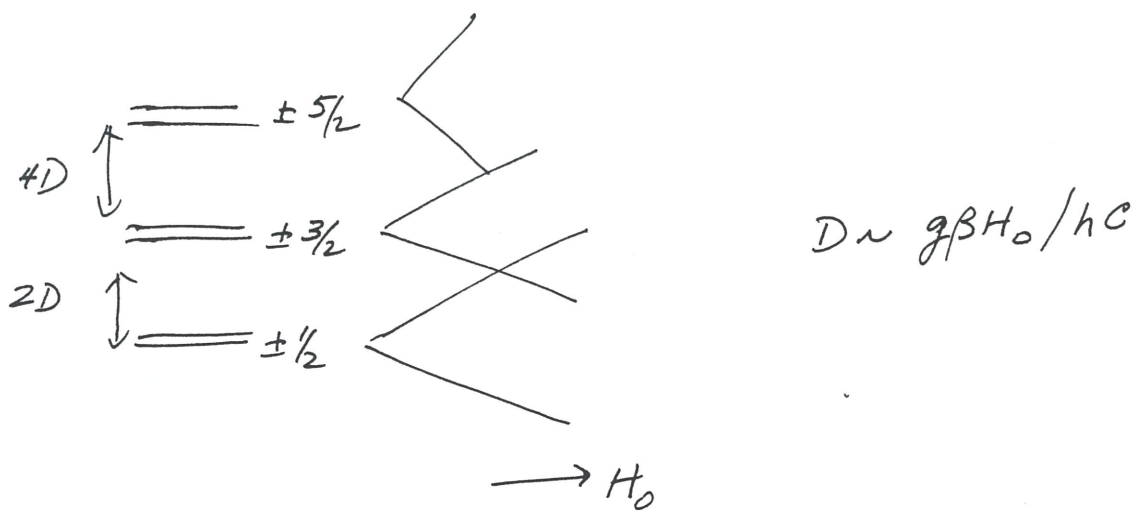
$g \approx 4$ when \vec{H} in xy plane
(triangular plane)

Powder Spectrum



derivative spectrum

(16)

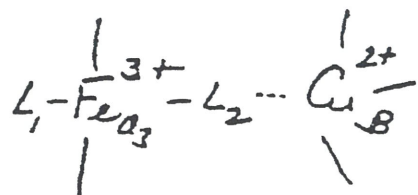
(b) Mn^{2+} high-spin d^5 D usually small $\sim 0.1 \text{ cm}^{-1} - 1 \text{ cm}^{-1}$ 

- Ligand Superhyperfine Interactions in EPR and ENDOR spectra provide more direct evidence of identity of ligands

(1) When ligand superhyperfine structure is large enough to be resolved in conventional EPR spectrum.

Illustrate this by way of the cytochrome a_3 , Cu_B cluster of cytochrome c oxidase.

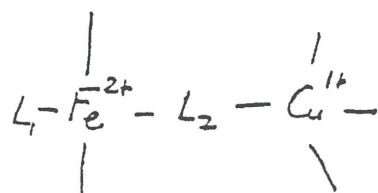
(a) Oxidized Cluster



high-spin
S=5/2 S=1/2 }
if L₂= H₂O, F⁻, formate Antiferromagnetic
Coupling \Rightarrow S=2
No conventional EPR!

low-spin
S=1/2 S=1/2 }
if L₂= OH⁻, CN⁻ S=0 antiferromagnetic
or 1 ferromagnetic

(b) Reduced Cluster



high-spin
S=2
if L₂= H₂O No conventional EPR!

low-spin
S=0
if L₂=CO,NO

No EPR for CO complex ; but NO is paramagnetic, so although NO-binding to iron heme convert Fe to low spin (S=0), the nitrosyl heme is an odd electron system with S=1/2

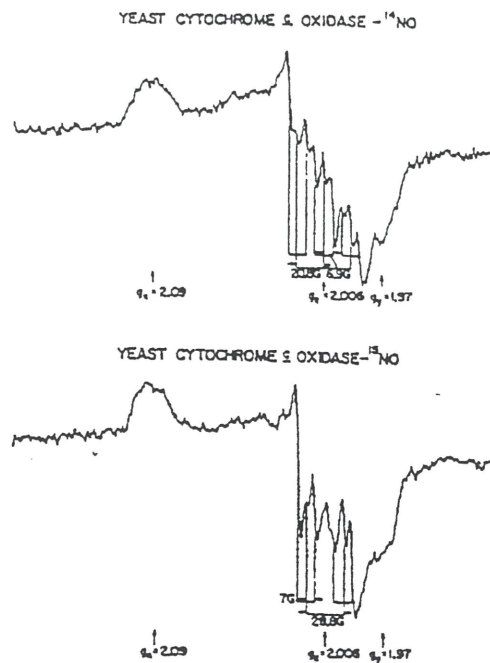
(c) EPR spectrum of ^{14}NO - and ^{15}NO adducts of reduced cytochrome c oxidase.

→ All 3 g-components are resolved

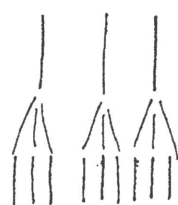
$$(g_1=2.09; g_2=2.006; g_3=1.97)$$

→ The $g=2.006$ component exhibits a (^{14}NO -adduct) nine-line hyperfine patterns, which can be interpreted in terms of the superposition of these sets of three lines arising from two nonequivalent nitrogens ($I=1$) interacting with the unpaired electron. The larger of the two hyperfine coupling constants is 20.8 Gauss and the smaller 6.9 Gauss.

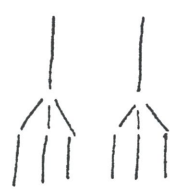
^{15}NO -adducts: When ^{15}NO is used in the experiment, the ^{15}NO -bound protein exhibits an EPR spectrum with g-value identical to those of the ^{14}NO -bound species, but the $g=2.006$ component shows a hyperfine pattern consisting of two sets of three lines. This pattern is consistent with the presence of one ^{14}N and one ^{15}N nitrogen bound axially to cytochrome a_3 with a 28.2 Gauss splitting for the ^{15}N and a 7.0 G splitting for the ^{14}N ligand.



Coupling to NO nitrogen



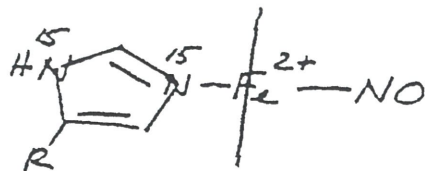
Coupling to second nitrogen



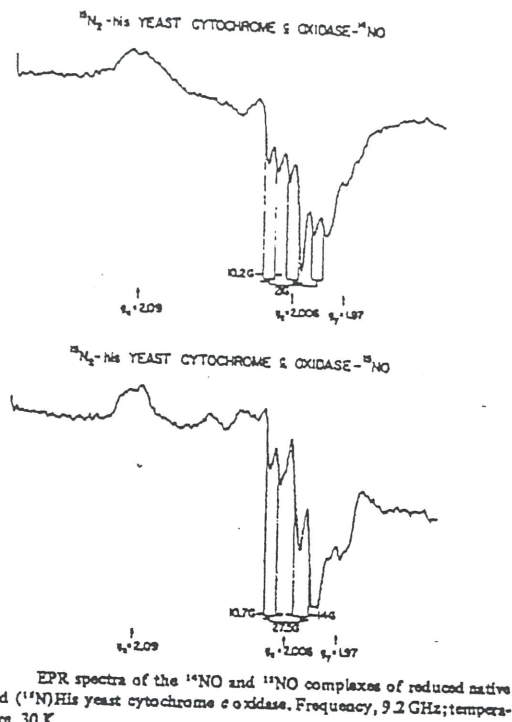
^{14}NO -adduct

^{15}NO -adduct

→ When experiment were repeated on a yeast cytochrome c oxidase preparation wherein all the histidines substituted with ^{15}N at both imidazole ring positions, the EPR spectra of the ^{14}NO - and ^{15}NO -adducts are altered.



The EPR spectra of the ^{15}NO - adduct of the (^{15}N) His protein consists of two sets of doublets, with a ^{15}NO nitrogen splitting of 27.5 Gauss and a splitting of 12 Gauss for the ^{15}N nitrogen of the histidine. The ^{14}NO -adduct exhibits a pattern consisting of 3 sets of doublets, with splitting of 21 Gauss to 10.2 G for the ^{14}NO and histidine ^{15}N nitrogen respectively.



EPR spectra of the ^{14}NO and ^{15}NO complexes of reduced native and (^{15}N)His yeast cytochrome c oxidase. Frequency, 9.2 GHz; temperature, 30 K.

→ These experiments provide unequivocal identification of histidine as the endogenous fifth ligand to cytochrome a_3 (in the reduced state).

(2) When ligand superhyperfine interaction is too small to be resolved in EPR spectrum

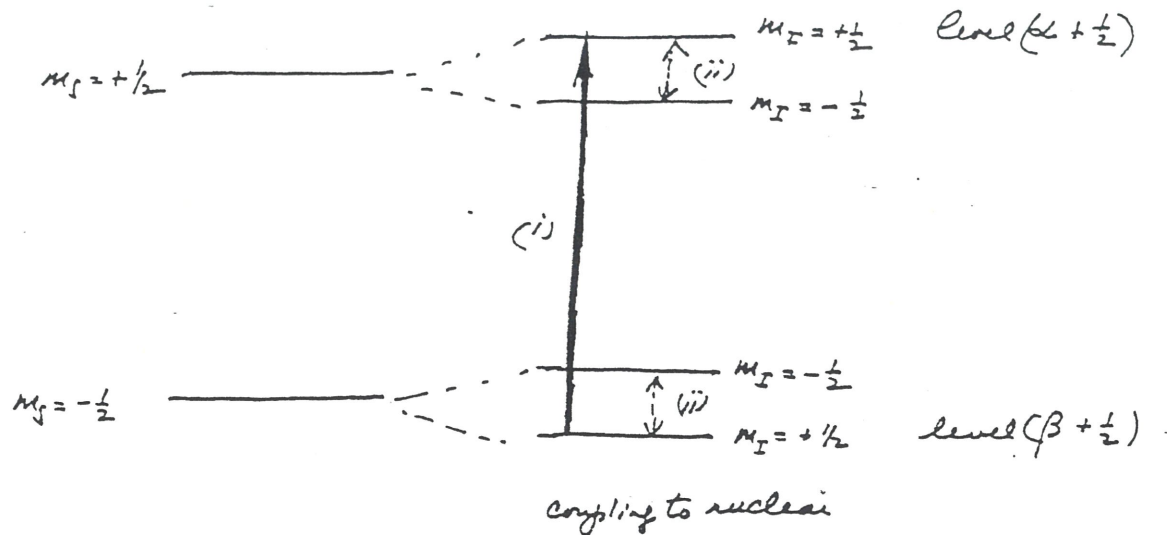
Appeal to ENDOR spectroscopy

≡ Electron Nuclear Double Resonance spectroscopy

Excite nuclear spins coupled to unpaired electron spin and use change in intensity of EPR spectrum to indicate resonance.

a) $I = \frac{1}{2}$ nucleus coupled to electron spin

Energy level diagram



(i) Saturated one of EPR transitions ($EPR \text{ intensity} = 0$)

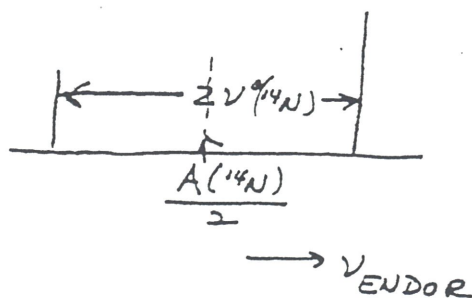
(ii) Slowly vary NMR frequency. At resonance, the population of level ($B + \frac{1}{2}$) will decrease, and population of level ($A + \frac{1}{2}$) will ~~increase~~ ⁱⁿ decrease. EPR will no longer be saturated and EPR intensity $\neq 0$.

(iii) The first order ENDOR spectrum of a nucleus of spin I consists of transitions at frequencies given by :

(a) When $\nu^0 = \text{NMR Larmor frequency} < A$

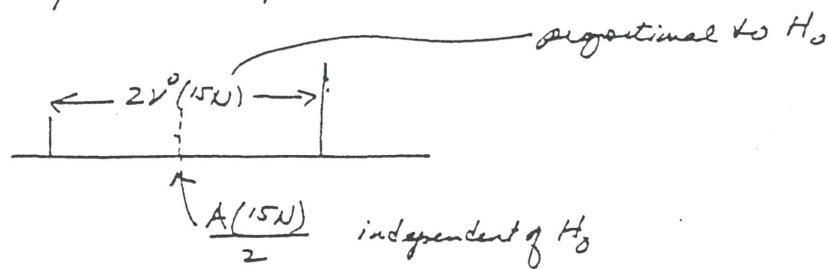
$$\nu_{\text{ENDOR}} = \frac{A}{2} \pm \nu^0$$

e.g. ^{14}N : a Larmor-split doublet centered at $\frac{A(^{14}\text{N})}{2}$ split by $\frac{1}{2}A(^{14}\text{N})$ (further splitting by electric quadrupole interaction)



^{15}N : a LaMour-split doublet centered at $A(^{15}\text{N})/2$
ad split by $\nu^o(^{15}\text{N})$.

(21)

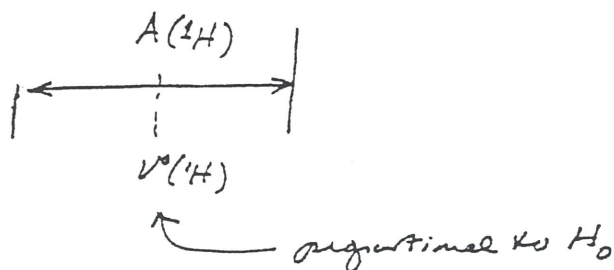


$$\text{note} \quad \frac{\nu(^{15}\text{N})}{\nu^o(\text{N})} = \frac{A(^{15}\text{N})}{A(^{14}\text{N})} = 1.403$$

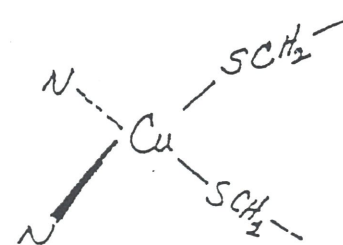
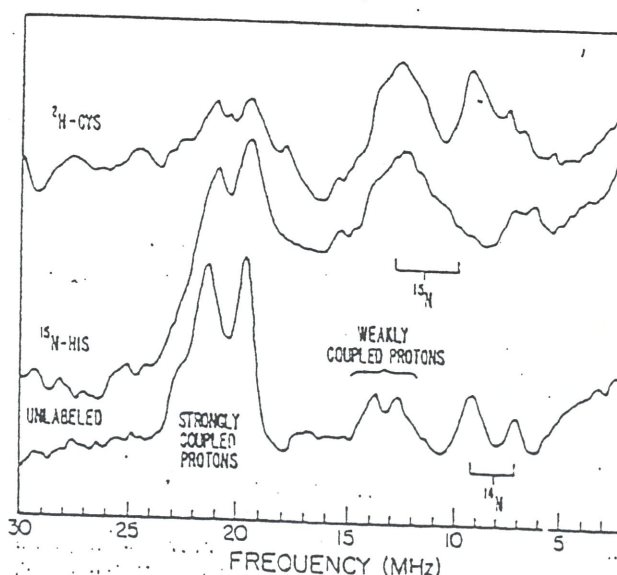
see page 14
for ENDOR at
two field
strengths

(b) When $\nu^o > A$ (e.g. ^1H)

$$\text{then } \nu_{\text{ENDOR}} = \nu^o(^1\text{H}) \pm \frac{A(^1\text{H})}{2}$$



(c) ^1H , ^{14}N and ^{15}N ENDOR of Cu_A site of cytochrome c oxidase



"Cu_A site"

ENDOR spectra of native, (^{15}N)His and (^3H)Cys yeast cytochrome c oxidase observed at $g = 2.04$, microwave frequency 9.12 GHz and temperature 2.1 K.

(22)

In the ENDOR of the Cax site, there are NMR signals assignable to ^{14}N , weakly-coupled protons, and strongly coupled protons for native yeast cytochrome c oxidase.

- ^{14}N signals are replaced by ^{15}N when the yeast is grown on ^{15}N -substituted (ring) histidine (98%)
- Strongly coupled protons disappear or attenuated in intensity when the yeast is grown on deuterated cysteine with 2H (>90%) at the β -carbon (β -methylene)
- These results provide unambiguous evidence for histidines and cysteines as ligands to Cax.

Ref: D.F. Blain et al, *Chemica Scripta* 21, 43-53 (1983);
T.H. Stevens & S.I. Chan, *J. Biol. Chem.* 256, 1069 (1981);
T.H. Stevens et al, *J. Biol. Chem.* 257, 12106 (1982)
T.H. Stevens, D.F. Bocie & S.I. Chan, *FEBS* 97, 314 (1979)